論文

A Study on the Coating Cracking on a Substrate in Bending I : Theory

Sung-Ryong Kim* and John A. Nairn**

굽힘모드하에서의 코팅크랙킹의 분석I : 이론

김성룡* · John A. Nairn**

ABSTRACT

The coating cracking on a substrate system was analyzed using a fracture mechanics approach. Multiple cracking in the bending configuration was analyzed using a variational mechanics approach to fracture mechanics of coating/substrate system. The strain energy release rate on bending geometry developed permits the prediction of crack growth in the coating layer on a substrate. Also, it can be used appropriately to the characterization of multiple cracking of coating. The obtained critical strain energy release rate (*in-situ* fracture toughness) will be a material property of coating and it will provide a better insight into coating cracking.

초 록

기재위에 입혀진 코팅에서 발생하는 크랙킹 현상을 파괴역학을 이용해서 분석하였다. 코팅/기재 구조에서 굽힘모드시 발생하는 코팅크랙킹을 변분법을 이용하여 분석하였으며, 본 연구에서 유도된 변위에너지 방출량을 통해 기재위에 입혀진 코팅층에서 크랙이 확장되는 것을 예측할 수 있다. 본 연구를 통해 얻어진 코팅의 임계 변위에너지 방출량은 재료의 고유성질이며 코팅크랙킹의 보다 근본적인 의미를 제공할 수 있다.

1. INTRODUCTION

Coatings are used in many applications such as in protection, decoration or alternation of the materials surfaces. In most cases the properties of applied coating is much different from the substrate or a free standing coating. Usually coatings are more brittle than the substrate to which they are applied. The differences make the coating/substrate system as an anisotropic and heterogeneous system. When a coating/substrate system is stressed, a crack will be formed in the coating layer. The crack will typically initiate and rapidly propagate through the entire thickness of the coating. When the crack reaches the coating/substrate interface, it has several alternative failure modes

* 삼양사 중앙연구소 화성소재Gr.
** Dept. of Materials Science and Engineering

[1,2], i.e. surface embrittlement, coating delamination, and multiple cracking. The three failure modes can be shown depending on the adhesion between coatings and substrates, mechanical properties of coating and substrate, residual thermal stresses, or interdiffusion of polymer chain into the substrate etc. For example an adhesion between coating and substrate can affect the failure mode [3]. Poor adhesion at the coating to substrate Interface shows coating delamination and good adhesion shows multiple cracking or surface embrittlement.

In this study the multiple cracking of coating in a bending configuration was considered. The coating crack can become arrested at the interface between coating and substrate. Further loading of the sample will cause additional cracks in the coating. If the coating cracks continue to be arrested, the result will be multiple cracks in the coating. Multiple cracking results in a delamination, degradation or surface embrittlement and is closely related to the coating's durability.

So far most of the studies of coatings were done on a free-film and not much studies were done on *in-situ* coating which is coating applied onto the substrate. The free-film test [4-6] do not accounts for adhesion and residual stress and the data obtained from a free-film test such as modulus and maximum strength do not give coatings fundamental criteria in real situation. In order to determine reliable coating properties for specific coating/substrate system all the factors including residual stresses should be included. Durelli and others used brittle coatings to analyze stress distribution in structures [7-10]. The phenomenon of brittle failure in high impact polystyrene caused by an application of a thin glassy polymer coating was studied [11-14].

The multiple cracking was analyzed here using a variational mechanics. An anisotropic property of coating/substrate system make us adapt cross-ply analysis in composite system. Previously we first analyzed the multiple cracking of coating of *in-situ* 3-layer coating/substrate system by adapting the composite microcracking on a tension geometry [1,2]. This paper is an extension of the previous analysis by considering bending geomety and multilayer system having n layers.

In this paper we have developed complementary energy of a multilayered sample upon bending geometry. Experimental verification of this analysis to fracture mechanics of *in-situ* multilayered coating system are reported in a companion paper [15].

2. FRACTURE MECHANICS ANALYSYS

Consider an undamaged multilayered sample having n layers under an arbitrary initial stress state in the x-z plane as illustrated in Fig. 1. The x direction is parallel to the axial direction of the layers and the z direction is transverse to the lay-

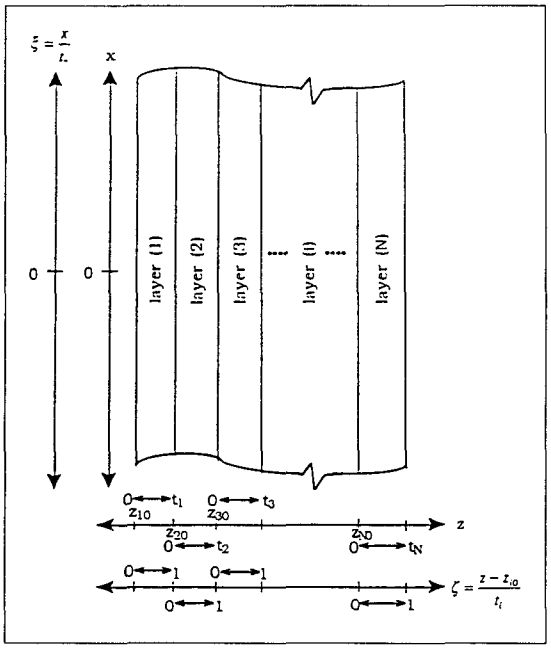

Fig. 1. The coordinate system of a multilayered sample has N layers. The axial direction is the x-axis and the thickness direction is the z-axis. The ξ and ζ directions are dimensionless directions located along the x- and z- axes, respectively

ers. The initial stress state (Φ) is defined using an initial stress function (ϕ) in dimensionless units ξ and ζ:

$$\Phi_0^{(i)}(\xi, \zeta) = t_i^2 \phi^{(i)}(\xi, \zeta) \quad (1)$$

where t_i is the thickness of layer i, the dimensionless x direction coordinate is $\xi = x/t_*$ where t_* is any conveniently chosen normalized length, and the dimensionless z direction coordinate is $\zeta = (z - z_{i_0}^{(i)})/t_i$, and where $z_{i_0}^{(i)}$ is the z coordinate at the start of layer i.

From the initial stress function, we derive the initial stress state as:

$$\sigma_{xx}^{(i)} = \frac{\partial^2 \Phi_0^{(i)}}{\partial z^2} = \frac{1}{t_i^2}\frac{\partial^2 \Phi_0^{(i)}}{\partial \zeta^2} = \frac{\partial^2 \phi_0^{(i)}}{\partial \zeta^2} = \phi_{\zeta\zeta}^{(i)} \quad (2)$$

$$\sigma_{xz}^{(i)} = -\frac{\partial^2 \Phi_0^{(i)}}{\partial x \partial z} = -\frac{1}{t_i t_*}\frac{\partial^2 \Phi_0^{(i)}}{\partial \xi \partial \zeta} = -\lambda_i \frac{\partial^2 \phi_0^{(i)}}{\partial \xi \partial \zeta} = -\lambda_i \phi_{\xi\zeta}^{(i)} \quad (3)$$

$$\sigma_{zz}^{(i)} = \frac{\partial^2 \Phi_0^{(i)}}{\partial x^2} = \frac{1}{t_*^2}\frac{\partial^2 \Phi_0^{(i)}}{\partial \xi^2} = \lambda_i^2 \frac{\partial^2 \phi_0^{(i)}}{\partial \xi^2} = \lambda_i^2 \phi_{\zeta\zeta}^{(i)} \quad (4)$$

where $\lambda_i = t_i/t_*$ and the subscripts on $\phi^{(i)}$ indicate partial differentiation with respect to the dimensionless variables.

When damage is introduced, the initial stress state will change. One and only one assumption is made: the change in the x-axis tensile stress in each layer is proportional to the initial x-axis tensile stress. The proportionality constant is a layer-dependent scaling function, $\Psi_i(\xi)$, that depends only on ξ and is independent of ζ. After damage the stresses become:

$$\sigma_{xx}^{(i)} = \phi_{\zeta\zeta}^{(i)}[1 - \Psi_i(\xi)] \quad (5)$$

A stress function that defines all possible stress states that satisfy this one assumption is

$$\Phi^{(i)}(\xi, \zeta) = t_i^2[\phi^{(i)}(\xi, \zeta)\{1 - \Psi_i(\xi)\} + \Psi_{i,a}(\xi)\zeta + \Psi_{i,b}(\xi)] \quad (6)$$

where $\Psi_{i,a}$ and $\Psi_{i,b}$ are two arbitrary functions of ξ only. The shear stress and z-axis tensile stress in the presence of damage becomes:

$$\sigma_{xz}^{(i)} = -\lambda_i[\phi_{\xi\zeta}^{(i)} - \frac{\partial}{\partial \xi}(\Psi_i \phi_\zeta^{(i)} - \Psi_{i,a})] \quad (7)$$

$$\sigma_{zz}^{(i)} = -\lambda_i^2[\phi_{\xi\xi}^{(i)} - \frac{\partial^2}{\partial \xi^2}(\Psi_i \phi^{(i)} - \Psi_{i,a}\zeta - \Psi_{i,b})] \quad (8)$$

Using boundary conditions and stress continuity conditions between layers and after defining functions $\omega_i(\xi, \zeta)$ and $\Psi_i(\xi)$ as :

$$\omega_i(\xi, \zeta) = \frac{\int_0^\zeta d\zeta' \int_0^\zeta d\zeta' \phi_{\zeta\zeta}^{(i)}}{\left\langle \phi_{\zeta\zeta}^{(i)} \right\rangle} \quad (9)$$

$$\Psi_i(\xi) = \Psi_i \left\langle \phi_{\zeta\zeta}^{(i)} \right\rangle \quad (10)$$

The new stress function in terms of these functions can be written as:

$$\Phi^{(i)} = t_i^2\left[\phi^{(i)} - \Psi_i \omega_i - \frac{1}{\lambda_i^2}\sum_{j=1}^{i-1} \lambda_j \Psi_j \left(\lambda_i \zeta + \lambda_{ji} + \lambda_j \left\langle \omega_{j,\zeta} \right\rangle\right)\right] \quad (11)$$

The general stress state is then

$$\sigma_{xx}^{(i)} = \sigma_{xx,0}^{(i)} - \Psi_i \omega_{j,\zeta\zeta} \quad (12)$$

$$\sigma_{xz}^{(i)} = \sigma_{xz,0}^{(i)} - \lambda_i \Psi'_i \omega_{j,\zeta} + \lambda_i \Psi_i \omega'_{j,\zeta} + \sum_{j=1}^{i-1} \lambda_j \Psi'_j \quad (13)$$

$$\sigma_{zz}^{(i)} = \sigma_{zz,0}^{(i)} - \lambda_i^2 \Psi''_i \omega_i - 2\lambda_i^2 \Psi'_i \omega'_i - \lambda_i^2 \Psi_i \omega''_i - \sum_{j=1}^{i-1}(\lambda_j \Psi''_j (\lambda_j \zeta + \lambda_{ji} + \lambda_j \left\langle \omega_{j,\zeta} \right\rangle, + 2\lambda_j^2 \Psi'_j \left\langle \omega'_{j,\zeta} \right\rangle + \lambda_j^2 \Psi_j \left\langle \omega''_{j,\zeta} \right\rangle) \quad (14)$$

where

$$\omega_{i,\zeta} = \frac{\partial \omega_i}{\partial \zeta} = \frac{\int_0^{\zeta} d\zeta \phi_{\zeta\xi}^{(i)}}{\left\langle \phi_{\zeta\xi}^{(i)} \right\rangle} \text{ and}$$

$$\omega_{i,\zeta\zeta} = \frac{\partial^2 \omega_i}{\partial \zeta^2} = \frac{\phi_{\zeta\xi}^{(i)}}{\left\langle \phi_{\zeta\xi}^{(i)} \right\rangle} \tag{15}$$

and superscripts ' and " represent partial differentiation with respect to ξ.

Using the subscript p to denote perturbation stresses, the stresses can be written

$$\sigma_{ij}^{(i)} = \sigma_{ij,0}^{(i)} + \sigma_{ij,p}^{(i)} \tag{16}$$

There are some constraints on the above stress state and therefore on the Ψ_i functions. For asymmetric problems there are x- and z- axes force balances, *x*- and z- axes moment balances, right edge shear stress boundary equation, and right edge transverse stress boundary condition.

If we consider multilayered samples loaded entirely by tractions (i.e. no displacement boundary conditions), the total complementary energy per unit depth is

$$\Gamma = \sum_{i=1}^{n} \frac{1}{2} \int_{x_i}^{x_f} dx \int_{z_0}^{z_f} d\vec{z}\vec{\sigma} \cdot \mathrm{K}^{(i)} \vec{\sigma}^{(i)}$$

$$= \sum_{i=1}^{n} \frac{\lambda_i t_*^2}{2} \int_{\xi}^{\xi_f} d\xi \int_0^1 d\zeta \vec{\sigma}^{(i)} \cdot \mathrm{K}^{(i)} \vec{\sigma}^{(i)} \tag{17}$$

where x_i, x_f, ξ_i, and ξ_f are the initial and final dimensioned and dimensionless coordinates of the area being considered and $K^{(i)}$ is the compliance tensor of the material in layer *i*. In the presence of damage, $\sigma^{(i)}$ is a sum of the initial stresses and the perturbation stresses. Hashin [16,17] showed that the complementary energy of any such cracked body can be written as

$$\Gamma = \Gamma_0 + \sum_{i=1}^{n} \frac{\lambda_i t_*^2}{2} \int_{\xi}^{\xi_f} d\xi \int_0^1 d\zeta \vec{\sigma}_p^{(i)} \cdot \mathrm{K}^{(i)} \vec{\sigma}_p^{(i)} \tag{18}$$

where Γ_0 is the complementary energy of the undamaged sample. This general result simplifies the analysis. To minimize the complementary energy of the damaged sample we can ignore the initial stress state which only contributes to the constant term Γ_0. We only need to minimize the stress energy calculated from the perturbation stresses.

2.1 Complementary Energy in an n=3, Asymmetric Problem with Initial Stresses Independent of x

The system used in this study was an asymmetric system of two layers, a thin coating on a thick substrate. The substrate was split into two layers to satisfy the boundary conditions, and discussions of this split (i.e. how to pick t_2 and t_3) can be found in ref. [1]. An x-z section of an asymmetric coated substrate with n = 3 is shown in Fig. 2. Layer 1 is the coating and it has modulus E_c and thickness t_1; layers 2 and 3 are in the substrate and they each have a modulus E_s and their thicknesses are t_2 and t_3.

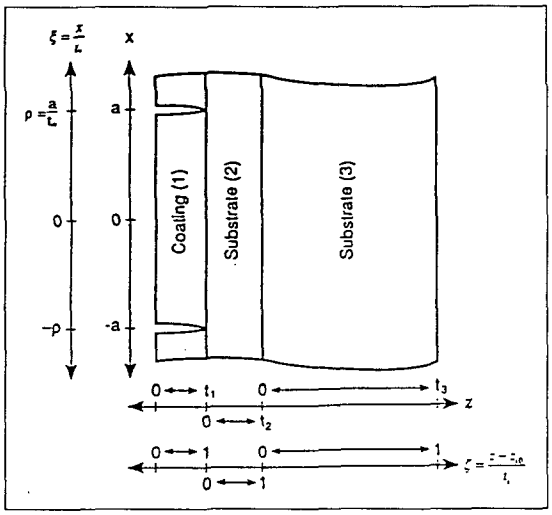

Fig. 2. The coordinate system between two cracks located at x=±a in the coating (layer 1). The substrate is divided into two layers - layers 2 and 3. The axial direction is the x-axis and the thickness direction is the z-axis. The ξ and ζ directions are dimensionless directions located along the x- and z- axes, respectively

For asymmetric systems, the final complementary energy is thus

$$\Gamma_p = t_*^2 \int_{\xi}^{\xi_f} d\xi (C'_1 \Psi_1^2 + C'_2 \Psi_1'' \Psi_1 + C'_3 \Psi_1''^2 + C'_4 \Psi_1'^2 + C'_5 \Psi_1' \Psi_1 + C'_6 \Psi_1'' \Psi_1') \quad (19)$$

where

$$C'_i = \lambda_1 C_{i,111} + C_{i,311} - \frac{\lambda_1 Q}{\lambda_2} C_{i,312} - \frac{\lambda_1 Q}{\lambda_2} C_{i,321} - \frac{\lambda_1^2 Q^2}{\lambda_2^2} C_{i,322} \quad (20)$$

$$Q = \frac{\lambda_1 \langle \omega_{1,\zeta} \rangle + \lambda_2 + \lambda_3 (1 - \langle \omega_{3,\zeta} \rangle)}{\lambda_2 \langle \omega_{2,\zeta} \rangle + \lambda_3 (1 - \langle \omega_{3,\zeta} \rangle)} \quad (21)$$

When the initial stresses are independent of x and therefore independent of ξ, all ξ derivatives of the ω_i functions will be zero. For this situation, eq. (19) becomes

$$\Gamma_p = t_*^2 \int_{\xi}^{\xi_f} d\xi (C'_1 \Psi_1^2 + C'_2 \Psi_1'' \Psi_1 + C'_3 \Psi_1''^2 + C'_4 \Psi_1'^2) \quad (22)$$

Each constant is evaluated. On normalization to layer 1, $\lambda_1 = 1$ is obtained. The constants C'_1 to C'_4 are as follows:

$$C'_1 = \frac{1}{2} \left[K_{xx}^{(1)} \langle \omega^2_{1,\zeta\zeta} \rangle + \frac{Q^2}{\lambda_2} K_{xx}^{(2)} \langle \omega^2_{2,\zeta\zeta} \rangle + \frac{(1-Q)^2}{\lambda_3} K_{xx}^{(2)} \langle \omega^2_{3,\zeta\zeta} \rangle \right] \quad (23)$$

$$C'_2 = K_{xz}^{(1)} (\langle \omega_{1,\zeta} \rangle - \langle \omega^2_{1,\zeta} \rangle) - K_{xz}^{(2)} Q (\lambda_2 (1 - (1+Q) \langle \omega_{2,\zeta} \rangle + Q \langle \omega^2_{2,\zeta} \rangle + \langle \omega_{1,\zeta} \rangle) - K_{xz}^{(3)} (1-Q) (\lambda_3 (1-Q) \langle (1 - \omega^2_{3,\zeta} \rangle + \lambda_2 (1 - Q \langle \omega_{2,\zeta} \rangle + \langle \omega_{1,\zeta} \rangle) \quad (24)$$

$$C'_3 = \frac{K_{xz}^{(1)}}{2} \langle \omega_1^2 \rangle + \frac{\lambda_2 K_{zz}^2}{6} \left[\lambda_2^2 (1 - 6Q \langle \omega_2 \zeta \rangle + 3Q^2 \langle \omega_2^2 \rangle) + 3 \langle \omega_{1,\zeta} \rangle (\lambda_2 + \langle \omega_{1,\zeta} \rangle - 2Q\lambda_2 \langle \omega_2 \rangle) \right] + \frac{\lambda_3 K_{zz}^{(3)}}{2} \left\{ \lambda_3^2 (1-Q)^2 \left(\frac{1}{3} - 2 \langle \omega_3 \zeta \rangle + \langle \omega_3^2 \rangle \right) + (\lambda_2 (1 - Q \langle \omega_{2,\zeta} \rangle) + \langle \omega_{1,\zeta} \rangle) \left[\lambda_2 (1 - Q \langle \omega_{2,\zeta} \rangle + \langle \omega_{1,\zeta} \rangle + \lambda_3 (1-Q) - 2\lambda_3 \langle \omega_3 \rangle (1-Q) \right] \quad (25)$$

$$C'_4 = \frac{1}{2} \left[K_{ss}^{(1)} \langle \omega^2_{1,\zeta} \rangle + \lambda_2 K_{ss}^{(2)} \langle (1 - \omega_{2,\zeta} Q)^2 \rangle + \lambda_3 K_{ss}^{(3)} (1-Q)^2 \langle (1 - \omega_{3,\zeta})^2 \rangle \right] \quad (26)$$

2.2 Initial Stresses Linear in z (Bending Loading Case)

In bending tests in which initial stresses are linear in z, the normal stresses ($\sigma_{xx,0}$) are given by

$$\sigma_{xx,0} = \frac{Mz}{I} \quad (27)$$

where M : bending moment of the beam
z : distance from the neutral surface
I : moment of inertia of the cross-section about the neutral axis.

Thus, as we can see from eq. (27), the initial normal stresses are linear in z and the following simplifications can be made :

$$\phi_{zz}^{(i)} = K^{(i)} (\zeta - C^{(i)}) \quad (28)$$

where $K^{(i)}$ is a layer dependent constant based on the maximum normal stress, and $C^{(i)}$ is a layer dependent constant normalized by the thickness of the ith layer.

From the definition of $\omega_i(\xi, \zeta)$, the following equations can be obtained

$$\omega_i = \frac{\frac{\zeta^3}{3} - C^{(i)} \zeta^2}{1 - 2C^{(i)}} \quad (29)$$

where $C^{(i)}$'s are constants defined as follows for n = 3

$$C^{(1)}=\frac{h_1}{t_1} \tag{30}$$

$$C^{(2)}=\frac{h_1-t_1}{t_2} \tag{31}$$

$$C^{(3)}=\frac{h_1-t_1-t_2}{t_3} \tag{32}$$

where h_1 is the distance from the neutral axis to the outer surface.

By substituting the above values into the equations (23)-(26), we can evaluate constants C'_1 to C'_4.

2.3 Variational Solution for Ψ

For thermoelastic analyses, a variational solution based on the principle of minimum complementary energy is found by minimizing the functional G given by:

$$\Gamma=\frac{1}{2}\int_V \sigma\cdot\mathbf{K}\sigma dV+\int_V \sigma\cdot\alpha T dV+\int_{S_1}\sigma\cdot\hat{u}dS \tag{33}$$

where σ is the stress tensor, **K** is the compliance tensor, α is the thermal expansion coefficient tensor, T is T_s ñT_0 (where T_s is the test temperature and T_0 is the stress-free temperature), V is the volume of the sample, and S_1 is that part of the sample subjected to a fixed displacement of û [18]. In this problem S_1 is null. Γ_p from eq. (33) modifies to

$$\Gamma_p=t_*^2\int_{\xi_i}^{\xi_j}d\xi(C_1\Psi^2+C_2\Psi'\Psi+C_3\Psi'^2+C_4\Psi^2+C_5\Psi'+C_6\Psi) \tag{34}$$

where

$$\Psi=\Psi_1,\ C_1=C_1',\ C_2=C_2',\ C_3=C_3',\ C_4=C_4',\text{ and } C'_6=-(\alpha_c-\alpha_s)T=-\Delta\alpha T \tag{35}$$

and C_5 is not needed because, from the boundary condition of zero shear stresses on the crack surfaces,

$$\int_{-\rho}^{\rho}\Psi'=0 \tag{36}$$

The result in eq. (34) is identical to the composite result in ref. [19] except that the constants C_1 through C_5 are different. The solution to the calculus of variation problem that yields Ψ can therefore be quoted directly from ref. [19]. The function Ψ that minimizes the complementary energy is

$$\Psi=\left(\sigma_{x0}^{(1)}+\frac{C_6}{2C_1}\right)\phi-\frac{C_6}{2C_1} \tag{37}$$

where ϕ is a function that depends on the sign of $4q/p^2-1$ where $p=(C_2-C_4)/C_3$ and $q=C_1/C_3$. When $4q/p^2$ is greater than 1:

$$\phi=\frac{2(\beta\sinh\alpha\rho+\cos\beta\rho+\alpha\cosh\alpha\rho\sin\beta\rho)}{\beta\sinh 2\alpha\rho+\alpha\sin 2\beta\rho}\cosh\alpha\xi\cos\beta\xi+\frac{2(\beta\cosh\alpha\rho\sin\beta\rho+\alpha\sinh\alpha\rho\cos\beta\rho}{\beta\sinh 2\alpha\rho+\alpha\sin 2\beta\rho}\sinh\alpha\xi\sin\beta\xi \tag{38}$$

where

$$\alpha=\frac{1}{2}\sqrt{2\sqrt{q}-p}\quad \beta=\frac{1}{2}\sqrt{2\sqrt{q}+p} \tag{39}$$

When $4q/p^2$ is less than 1 (and $p<0$ and $q>0$):

$$\phi=\frac{\beta\cosh\alpha\xi}{\sinh\alpha\rho\,(\beta\coth\alpha\rho-\alpha\coth\beta\rho)}+\frac{\alpha\cosh\beta\xi}{\sinh\beta\rho\,(\alpha\coth\beta\rho-\beta\coth\alpha\rho)} \tag{40}$$

where

$$\alpha=\sqrt{-\frac{p}{2}+\sqrt{\frac{p^2}{4}-q}},\ \beta=\sqrt{-\frac{p}{2}-\sqrt{\frac{p^2}{4}-q}} \tag{41}$$

One feature of the coatings analysis that differs from the composite analysis in ref. [19] is that we must choose where to divide the substrate layer into two separate layers. The minimum complementary energy is produced when the zone of stress disturbance is about the same size as the crack [1] or when the thickness of layer 2 is equal to the thickness of the coating. Under this condition

$$\lambda_1 = \lambda_2 = 1,\ \lambda_3 = \lambda \text{ and } R = \frac{2}{1+\lambda} \tag{42}$$

and the expressions for C_1 through C_4 in eqs. (23) - (26) can be simplified.

2.4 Energy Release Rate for a Crack in the Coating

Before starting on the multiple cracking fracture analysis, we give three useful results from ref. [19]. Consider the sample A in Fig. 3 with N crack intervals characterized by crack spacings ρ_1, ρ_2, ρ_3,$\cdots$, ρ_N. The sample compliance is

$$C = C_0 + \frac{E_c^2}{E_0^2}\frac{2C_3 t_1 L}{B^2 W}\frac{\sum_{i=1}^{N}\chi(\rho_i)}{\sum_{i=1}^{N}\rho_i} \tag{43}$$

where $B = t_1+t_2+t_3$ is the total thickness, W is the sample width, L is the sample length and $C_0 = L/(BE_0W)$ is the compliance of the uncracked sample. The new function $\chi(\rho)$ depends on the sign of $4q/p^2-1$. When $4q/p^2$ is greater than 1:

$$\chi(\rho) = 2\alpha\beta(\alpha^2+\beta^2)\frac{\cosh 2\alpha\rho - \cos 2\beta\rho}{\beta\cosh 2\alpha\rho + \alpha\sin 2\beta\rho} \tag{44}$$

when $4q/p^2$ is less than 1:

$$\chi(\rho) = \alpha\beta(\beta^2-\alpha^2)\frac{\tanh\beta\rho - \tanh\alpha\rho}{\beta\tanh 2\alpha\rho - \alpha\tanh\alpha\rho} \tag{45}$$

The total strain energy (U) in the N crack intervals is

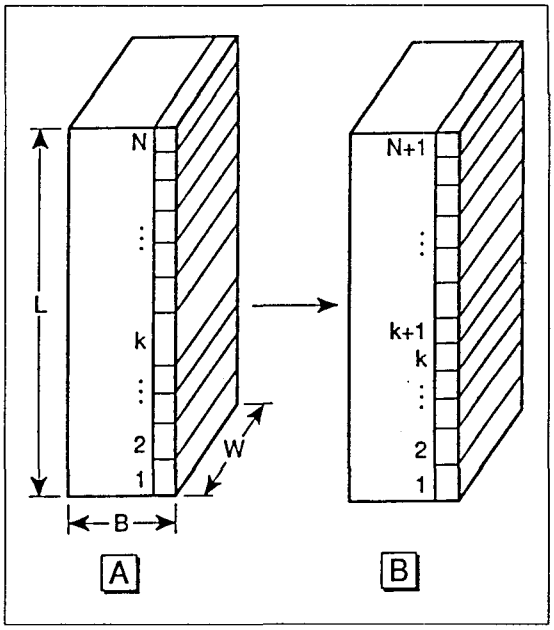

Fig. 3. Sample A has N cracks with crack spacings ρ_1, ρ_2,$\cdots$,ρ_N. (b) Sample B has a new crack located in the kth crack interval of sample A. Sample length (L), thickness (B), and width (W) are shown on sample A

$$U = \left(\frac{\sigma_0^2}{2E_0} + \frac{t_1 C_6^2}{4C_1 B}\right) BWL + (C-C_0)\frac{E_0^2}{E_c^2}\frac{B^2W^2}{2}\left(\frac{E_0^2}{E_c^2}\sigma_0^2 - \frac{C_6^2}{4C_1^2}\right) \tag{46}$$

Finally, the longitudinal thermal expansion coefficient (α_L) of the cracked sample is

$$\alpha_L = \alpha_L^0 - \frac{C-C_0}{C_0}\frac{\Delta\alpha}{2C_1E_c} \tag{47}$$

where α_L^0 is the thermal expansion coefficient of the uncracked sample.

By the energy approach to multiple cracking in coatings, we assume that the next coating crack will form when the energy released on forming that crack reaches the fracture toughness of the coating. Consider the formation of a crack in the

kth interval as shown in Sample B Fig. 3. The energy release rate on forming this crack can be found by differentiating eq. (46) with respect to total crack area, A, at constant displacement [19]:

$$G = -\frac{dU}{dA}\Big|_{const.u} = \frac{E_0^2}{E_c^2}\frac{B^2W^2}{2}\left(\frac{E_0}{E_c}\sigma_0+\frac{C_6}{2C_1}\right)^2\frac{dC}{dA} \quad (48)$$

In deriving eq. (48) we need to evaluate $d\sigma_0/dA|_{const.\,u}$. Using the relation for sample compliance (C) times load (P):

$$CP = u(P)-u(0) = u(P)-\alpha_1 LT \quad (49)$$

where u(P) is the sample displacement under a load P, and differentiating results in

$$\frac{d\sigma_0}{dA}\Big|_{const.u} = \left(-\frac{\sigma_0}{C}+\frac{E_0}{E_c}\frac{\Delta\alpha T}{2C_1C}\right)\frac{dC}{dA} \quad (50)$$

Evaluating dC/dA by differentiating eq. (43) results in the final energy release rate expression:

$$G = \left\langle\sigma_{xx,0}^{(1)}\right\rangle^2 C_3 t_1 Y(D) \quad (51)$$

In bending, the average normal stress in the first layer (coating layer) of a multilayer system is given by

$$\left\langle\sigma_{xx,0}^{(1)}\right\rangle = \frac{2\bar{z}_1}{B}E_{xx}^{(1)}\xi_{max} \quad (52)$$

and $\bar{z}_1$ is average distance from neutral axis of sample to the first layer and $\xi_{max} = \frac{MB}{2E_0I}$ where M is the bending moment applied to the beam, B is the thickness of the sample and I is the moment of inertia of the entire sample.

Y(D) in eq. (51) is a calibration function that depends on the crack density, D = N/L, or more formally on the complete distribution of crack spacings:

$$Y(D) = LW\frac{d}{dA}\frac{\sum_{i=1}^{N}\chi(\rho_i)}{\sum_{i=1}^{N}\rho_i} = 2\frac{d}{dD}\left(D\langle\chi(\rho)\rangle\right) \quad (53)$$

where $\langle\chi(\rho)\rangle$ is the average value of $\chi(\rho)$ over the N crack spacings.

In order to use eq. (51), we must evaluate Y(D). For the fracture process illustrated in Fig. 3 where a new crack forms in the center of the kth interval, we can evaluate Y(D) using discrete differentiation. Before the crack forms $\langle\chi(\rho)\rangle = \frac{1}{N}\sum_{i=1}^{N}\chi(\rho_i)$ and D = N/L. After the crack forms $\langle\chi(\rho)\rangle = \frac{1}{(N+1)}\sum_{i=1}^{N}(\chi(\rho_l)-\chi(\rho_k)+2\chi(\rho_k/2))$ and D = (N+1)/L. The calibration function is then:

$$Y(D) = 2\frac{\Delta(D\langle\chi(\rho)\rangle)}{\Delta D} = 2(2\chi(\frac{\rho_k}{2})-\chi(\rho_k)) \quad (54)$$

During a typical experiment we will not know the location of the next crack. Because during multiple cracking cracks tend to form regular arrays, we assume that the next crack will form in a crack interval whose spacing is close to the average spacing. In other words when the crack density is D, the next crack will form in a crack interval whose spacing is $\rho = 1/(2t_1D)$ and the calibration function is given by

$$Y(D) = 2\chi\left(\frac{\rho}{2}\right)-\chi(\rho) = 2\chi\left(\frac{1}{4t_1D}\right)-\chi\left(\frac{1}{2t_1D}\right) \quad (55)$$

Finally, we consider the formation of the first

crack. The energy release rate for the first crack is

$$G = \left\langle \sigma^{(1)}_{xx,0} \right\rangle^2 C_3 t_1 \lim_{D\to 0} Y(D) \tag{56}$$

For the two solutions described above, when $4q/p^2$ is greater than 1:

$$\lim_{D\to 0} Y(D) = 2d\sqrt{\frac{C_1}{C_3}} \tag{57}$$

and when $4q/p^2$ is less than 1:

$$\lim_{D\to 0} Y(D) = (\alpha+\beta)\sqrt{\frac{C_1}{C_3}} \tag{58}$$

The strain energy release rate on bending geometry developed permits the prediction of crack growth in the coating layer on a substrate. Figure 4 is a schematic prediction of crack density vs. applied strain for thinner and thicker coating on a metallic substrate using eg. (56). It gives a key feature of experimental results. The thicker coating starts to crack first than thinner coating but the number of coatings will saturate at lower strain value. On the other hands, the thinner coating shows the first crack at a higher strain value and it reaches a higher crack density. The cracks formed sooner in thicker coatings because each crack released more energy than the crack in a thinner coating. It is well known in the coating industry that the thicker coating shows a crack sooner [7]. The developed fracture mechanics theory was agreed qualitatively with the experimental works [7,15].

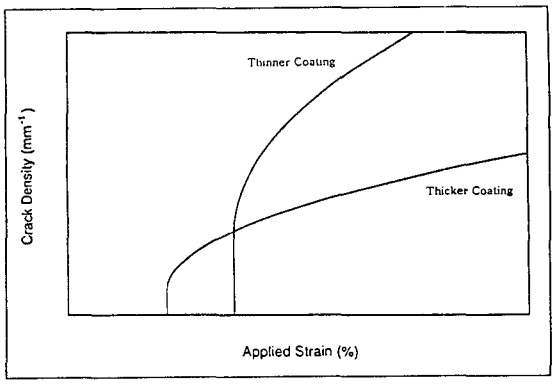

Fig. 4. Schematic theoretical predictions of crack density vs. applied strain for thin and thick coating

3. CONCLUSIONS

We have derived an energy release rate for multiple cracking in a coating layer on a multilayered system using a variational mechanics. A crack density information as a function of strain could be used to get the *in-situ* fracture toughness of coatings. If coating shows multiple cracking then we might expect the failure to occur at a critical value of the critical multiple cracking strain energy release rate. In other words, when the stress reaches increases to a level such that $G = G_C$, coating multiple cracking would occur. The measured critical strain energy release rate (G_C) would be a fracture toughness of that coating and it is a physically meaningful material property.

REFERENCES

1. J. A. Nairn and S.R. Kim, *Engng Fracture Mech.* **42**, 195 (1992).

2. S.R. Kim, *Fracture Mechanics Approach to Multiple Cracking in Paint Films*, Master's Thesis, University of Utah, 1989.

3. T.C. Gilmer and P.L. Adesko, AICHE Symposium Series, **84**, 260 (1988).

4. ASTM D-2370, *Tensile Properties of Organic Coatings* (1982).

5. G. G. Sward, editor, *Paint Testing Manual*, ASTM STP 500, 1 (1972).

6. J. Ahn, K. L. Mittal, and R. H. MacQeen, ASTM STP 640 (1978).

7. A. J. Durelli, E.A. Phillips and C. H. Tsao, *Introduction to the Theoretical and Experimental Analysis of Stress and Strain*, Chapter 16,

McGraw-Hill, New York, 1958.

8. A.V. Forest and G. Ellis, J. Aeronautical Sci. **7**, 205 (1939)

9. J. S. Caswell, *Metallurgia*, **41**, 165 (1950).

10. J. R. Linge, D.C.Ae., and A.F.R.Ae.S., *Aircraft Engng*. 94 (1958).

11. P. So and L. J. Broutman, *Polym. Engng Sci.* **22**, 888 (1982).

12. L. Rolland and L. J. Broutman, *Polym. Engng Sci.* **25**, 207 (1985).

13. R. O. Carhart, D. A. Davis and R. Giuffria, *SPE Jl*, April, 440 (1962).

14. L.Y. Xu, *Engng Fract. Mech.* **156**, 827 (1997).

15. S.R. Kim and J.A. Nairn, *J. Kor. Soc. for Com. Mat.* Submitted.

16. Z. Hashin, *Mech. Mater.* **4**, 121 (1985).

17. Z. Hashin, *Engng Fracture Mech.* **25**, 771 (1986).

18. D.E. Carlson, in *Mechanics of Solids* (Edited by C. Truesdell), Vol. II, p325, Springer-Verlag, Berlin, 1984.

19. J. A. Nairn, *J. Compos. Mater.* **23**, 1106 (1989).